

SECTION III:

INTERFEROMETRY

SPECKLE INTERFEROMETRY WITH THE BTA TELESCOPE

V.N. Dudinov, V.V. Konichek, S.G. Kuz'menkov, V.S. Tsvetkova
V.S. Rylov,* L.V. Gyavgyanen,* and V.N. Erokhin*
Astronomical Observatory of Khar'kov University
* Special Astrophysical Observatory USSR AS

ABSTRACT: The description of a speckle camera used with the BTA 6-meter telescope is given. Observational data recorded on photographic film are processed with a Fourier optical spectrum analyzer. Results of binary star measurements are presented. Analysis of short exposure images of a point source obtained with telescopes of various sizes allows the estimation of atmospheric parameters which are necessary for correct application of speckle interferometry.

1. INTRODUCTION

In 1977 a programme of speckle interferometric measurements with the BTA 6-meter telescope was started by joint efforts of the Special Astrophysical Observatory of the USSR Academy of Sciences and the Astronomical Observatory of Khar'kov University. Before 1979, speckle images of some bright stars were recorded directly on film, Isopanochrome T-22, without an image intensifier. Some results of these experiments have been reported by Dudinov et al. (1979, 1980). It was shown that in some cases the spectral range could be considerably expanded as compared to that usually accepted. For $\Delta\lambda = 100\text{nm}$ and a 30ms exposure the extreme stellar magnitude was 1^m. It was under these conditions that the angular diameter of α Tau was measured (Dudinov et al. 1980). Since March 1979 observations have been performed with a speckle camera which included a UM-92 image tube.

2. BTA SPECKLE CAMERA

At present the BTA speckle equipment (Figure 1) is mounted at the Nasmyth focus (focal length 173m) and includes an image intensifier, a filter assembly, an atmospheric dispersion compensator, and a camera.

2.1 Atmospheric dispersion compensator

The compensator consists of two prisms 70mm in diameter. The first

prism is made of flint glass F1 with a refraction angle $9^{\circ}00'$ and the other is made of heavy crown glass TK 14 with a refraction angle $9^{\circ}01'$. The compensator is mounted on the exit flange of the Nasmyth focus. While changing the zenith distance, the exit flange rotates synchronously so that the axis of the compensator always coincides with that of the atmospheric dispersion. The amount of compensation is varied by moving the prisms along the beam. The compensator removes the effect of atmospheric dispersion with an accuracy exceeding the diffraction limit of the telescope for the range of zenith distances 15° – 60° and spectral bandwidth 40nm.

2.2 Filter assembly

The filter assembly consists of two disks one of which carries interference filters with passband maxima 560nm, 600nm, and 650nm, and a half-width $\Delta\lambda = 40$ nm. The other disk carries interference filters with a half-width 10–15nm. These filters are chosen for observations of cool stars in the continuum ($\lambda = 610$ nm) and in TiO absorption bands ($\lambda = 590$ nm and 623nm). In addition to a neutral density filter there are also two red glass filters on the same disk, which, together with an image tube photocathode, provide a passband 100–150nm in the far red part of the spectrum.

2.3 Image intensifier

The intensification of speckle images is accomplished using a three stage magnetically focused image tube UM-92 with a multialkali photocathode. The sensitivity maximum is at 500nm and the cutoff is at 850nm. For the tube used until 1981, the intensifier luminosity gain

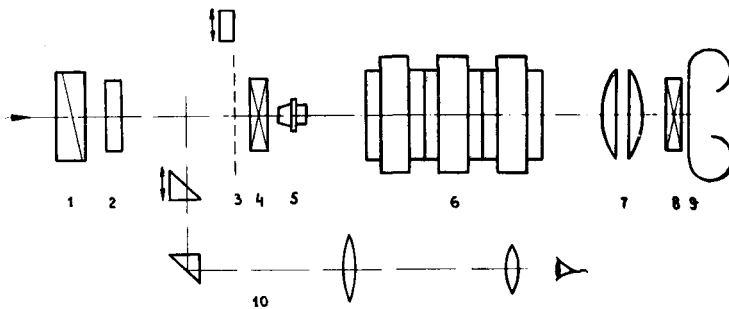


Figure 1. BTA speckle camera: 1) atmospheric dispersion compensator, 2) filter assembly, 3) telescope focal plane, 4) mechanical shutter, 5) microscope objective, 6) image intensifier, 7) transfer optics, 8) camera shutter, 9) recording plane, 10) viewfinder system.

was 10^3 with a photocathode operating field diameter of 15mm, resolution 10mm^{-1} and screen persistence (decay to 10%) 15ms. The system incorporates a mechanical shutter together with a variable camera shutter, permitting a range of exposures from 3 to 30ms. In 1981 another three stage image tube with a multialkali photocathode and magnetic focusing was used. The luminosity gain of this is $5 \cdot 10^3$, the photocathode effective diameter is 20mm, and the resolution is 15mm^{-1} on the film.

2.4 Image scale and calibration

The equivalent focal distance of the entire system (telescope + speckle camera) may be varied from 480 to 550m. To calibrate the speckle camera scale and to check the image intensifier resolution, a hatched, absolute contrast target is usually photographed during observations. Accuracy of the speckle camera scale determination is not worse than 0.1%. For position angle calibration, details of the telescope construction projected at the exit pupil plane are photographed. Because of the altazimuth mounting, these details do not change their orientation around the horizon.

2.5 Recording

A 35mm picture camera is mounted at the speckle camera output. The film holder capacity is 60m. Recording is carried out on Isopan-chrome T-22 film with resolution 120mm^{-1} and a rate of 5 frames per second. As many as 150-200 frames are usually recorded for double stars and 250-300 frames for angular diameter measurements.

3. PROCESSING OF SPECKLE IMAGES

Statistical processing of observational data is made with a coherent optical spectrum analyzer of the Khar'kov University (Dudinov et al., 1977). The spectrum analyzer has two plano-convex lenses with an immersion liquid between them where the film is transported. The low aperture ratio and the minimal number of optical surfaces almost entirely exclude both the aberrations and coherent noise effects at the spectrum analyzer output.

Coherent optical techniques are commonly believed to yield intrinsically low accuracy. However, our experience has shown that the accuracy of processing is determined only by the properties of the photodetector at which the initial image is recorded. For existing panoramic photodetectors, noise and non-linearity of the dynamic response (or the error of its measurement) are so considerable that the full potential for high accuracy with a digital system and an optical processor is not realized in practice. To estimate the nonlinearity of a signal introduced into the coherent optical processor, special tests are used which allow the value of the non-linearity to be estimated from the spectrum directly. Selected development regimes ensure linearity with an accuracy better than 1% for the 50 times intensity range.

Careful photometric control and the high technical characteristics of the spectrum analyzer make it possible to process data with the accuracy required to perform one of the most demanding applications of speckle interferometry, i.e. measurements of stellar angular diameters (Dudinov et al., 1979).

Measurements of power spectra of binaries are usually performed with a universal measuring microscope. In the case of low fringe visibility, standard photometric processing is performed followed by a numerical division over a point source power spectrum.

4. RESULTS

Results of some binary star measurements made in 1980 are presented in Table 1 to illustrate the accuracy of our measurements. Comparison of results for the same object obtained with various filters (ADS 3841, ADS 4890) or various exposures (ADS 11149) and results from observations separated by several days (objects with slow orbital motion, ADS 11468, QS Aql) shows their high stability. The internal errors are $\sim 1\%$ for component separations and 0.1° for position angles. Comparison with the ephemeris calculated for orbits from the "Third Catalogue of Orbits of Visual Binary Stars" (Finsen and Worley, 1970), shows that there are no systematic deviations. Residuals between the present observations and the ephemeris calculations are given in columns 5 and 7 of Table 1. Note that the system ADS 11149 has not been identified as being triple in previous speckle interferometric measurements.

5. STRUCTURE OF SHORT EXPOSURE IMAGES AND ATMOSPHERIC CHARACTERISTICS

Analysis of short exposure images of a point source gives all necessary information about the atmosphere as a random medium distorting astronomical images, and permits estimation of the spectral range and angular distance between two point sources for which correlation is still perceptible. According to present views based mainly on the works of V.I. Tatarski and D. Fried, distortions of an astronomical image are completely described by the parameters of a turbulent medium satisfying the Kolmogorov-Obukhov law. In this case the autocorrelation function of a plane wave passing through a turbulent medium is

$$C(\rho) = \exp\{-3.44(\rho/r_0)^{5/3}\},$$

where ρ is the separation distance and r_0 is the Fried parameter completely representing image quality.

However, statistical properties of the real atmosphere may differ considerably from the Kolmogorov-Obukhov law which applies to a free atmosphere. Image formation is critically affected by different factors, especially by conditions inside and around the dome. In our opinion, agreement of the theory with experiment is due to the fact that

ADS	Epoch (1980.0+)	λ (nm)	Separation (milliarcsec)	Residual	Position Angle (degrees)	Residual
γ Per	0.7745	600	200 \pm 3		63.3 \pm 0.3	
3841Ap	0.7829	650	47 \pm 1	0	180.8 \pm 0.5	+ 2.1
	0.7993	590	43 \pm 1	+ 1	157.7 \pm 0.5	+ 2.0
	0.7993	610	43 \pm 1	+ 1	157.7 \pm 0.5	+ 2.0
4229AB	0.7773	560	82 \pm 1	+ 5	68.7 \pm 0.3	+ 1.7
4265	0.7773	560	340 \pm 2	+165	236.6 \pm 0.3	-14.5
Rst5225	0.7828	560	230 \pm 4	+ 28	203.0 \pm 0.3	-28.6
4890Ap	0.7828	600	100 \pm 1	+ 38	110.8 \pm 0.4	-49.1
	0.7828	560	98 \pm 1	+ 36	110.5 \pm 0.4	-49.4
6185AB	0.7828	600	147 \pm 1		329.3 \pm 0.3	
10 UMa	0.7993	600	737 \pm 6	+ 38	18.8 \pm 0.2	- 1.1
7158	0.7883	560	292 \pm 2	+ 38	284.9 \pm 0.2	+ 2.3
8804AB	0.4205	600	529 \pm 4	+ 42	191.2 \pm 0.3	- 0.3
9744AB	0.4153	560	213 \pm 2	+ 3	67.7 \pm 0.3	- 1.6
				+ 4		- 1.8
	0.4264	600	213 \pm 3	+ 3	68.6 \pm 0.4	- 0.7
				+ 4		- 0.9
10360AB	0.4182	560	98 \pm 1	- 72	78.4 \pm 0.4	- 8.0
				- 23		+19.8
				- 17		+ 1.6
	0.4264	560	97 \pm 6	- 72	77.7 \pm 0.8	- 8.7
				- 24		+19.3
				- 18		+ 1.1
11149AB	0.7870	560	98 \pm 1		44.2 \pm 0.4	
AB,C			750 \pm 12		216.5 \pm 0.5	
AB	0.7870	560	97 \pm 1		44.1 \pm 0.4	
AB,C			756 \pm 10		216.5 \pm 0.3	
11468	0.4183	560	270 \pm 2	- 57	93.5 \pm 0.3	+ 1.2
				- 49		+ 5.8
	0.4265	560	272 \pm 3	- 55	94.9 \pm 0.4	+ 2.6
				- 47		+ 7.2
QS Aql	0.7761	560	163 \pm 2		306.2 \pm 0.3	
	0.7871	560	164 \pm 2		306.6 \pm 0.4	
15032Aa	0.4185	650	184 \pm 3		49.2 \pm 0.3	

Table 1. Binary star measurements

the values being measured depend weakly on the accepted statistical model of light wave distortions rather than good accordance of real conditions with the Kolmogorov-Obukhov law.

The main conclusion of turbulence theory is the absence of any characteristic size of turbulent irregularities. The process describing phase fluctuations of a plane wave passing through a turbulent medium is a random one with stationary first deviations (a lack of stationarity

prevents a sampling interval for the function representing phase fluctuations from being introduced and the characteristic size then appears only as a correlation radius of the distorted light wave).

When studying a series of instantaneous images it may be reasonable to abandon the generally used model and to treat the distortions of the plane wave phase as a random function which belongs to a stationary random process. That means that we ignore possible correlation at distances significantly exceeding the telescope diameter.

An instantaneous image of a point source $g(x,y)$ is described by the equation:

$$g(x,y) = \left| \iint_G \exp\{i\phi(\xi,\eta)\} \exp\{-i\frac{2\pi}{\lambda F}(x\xi+y\eta)\} d\xi d\eta \right|^2 \quad \text{---(1)}$$

where G is the region occupied by the telescope entrance pupil; ξ, η and x, y are co-ordinates in the pupil plane and the focal plane, respectively; F is the focal distance. The absence of a distinct maximum in the image of a point source is evidence of a deep phase modulation. It means that the spatial spectrum of the function $\phi(\xi, \eta)$ may be much narrower than the spectrum of the function $\exp\{i\phi(\xi, \eta)\}$ determining the size of the image $g(x, y)$. Let the instantaneous realization of $\phi(\xi, \eta) = (2\pi/\lambda) \cdot h(\xi, \eta)$ at the aperture be represented by a polynomial $(2\pi/\lambda) \cdot P(\xi, \eta)$, whose coefficients for fixed n minimize the squared deviation of the polynomial from function $\phi(\xi, \eta)$. For a given approximation error, e.g. $\pi/2$, the power of the polynomial is determined by the wavelength and the entrance pupil size. When the size of the entrance pupil $D \ll d_0$, where d_0 is the Nyquist interval of function $h(\xi, \eta)$, then $h(\xi, \eta) = a_0 \xi + b_1 \eta$. According to (1) the image in this case is diffraction limited with its co-ordinates determined by the instantaneous phase slope. The image position does not depend on wavelength and therefore the instantaneous image structure does not depend on the phase slope value over the spectral interval $\Delta\lambda$.

For aperture sizes comparable with the Nyquist interval, $D \leq d_0$, a quadratic approximation is sufficient. By proper co-ordinate rotation and translation, the function $h(\xi, \eta)$ can be represented as

$$h(\xi, \eta) = a_2 (\xi - \xi_0)^2 + b_2 (\eta - \eta_0)^2$$

A quadratic phase shift means defocusing, with astigmatism in the case when coefficients a_2 and b_2 are unequal. In the case of central symmetry ($a_2 = b_2$), a quadratic phase distortion of λ over the aperture size causes image defocusing with the energy concentrated in a circle of diameter twice the diffraction diameter and zero intensity in its centre. For arbitrary coefficients a_2 and b_2 with phase distortion not more than λ , the power spectrum of such images has an excess at the spatial frequency which corresponds to doubling (Chernyj, 1980). For the 70cm telescope of the Khar'kov Observatory such doubling is usually observed in red light. Doubling disappears with a green filter. For

the 60cm telescope at Mount Maidanak (elevation approximately 3000m) doubling remains in visual light and disappears only in the ultraviolet. From these data the lower limit of the maximum wave front curvature can be estimated as $5 \times 10^{-8} \text{ cm}^{-1}$. The maximum value of phase slope can be taken as $1''$. Using the Bernstein inequality, which connects the maximum value of the function derivative with its spectral band, one can obtain for the phase correlation radius the estimate $a_1/a_2 \sim 1\text{m}$. Over this interval, deviation of the function $h(\xi, \eta)$ from its average does not exceed 2λ . The same deviation value must be expected also for apertures $D \gg d_0$.

For fine structure to exist in an instantaneous image (i.e. for proper time coherence) the spectral band-width of the speckle camera for the 6m telescope must not exceed $\lambda/4$. This allows us to increase the energy throughput by expanding the passband to 150nm. It is noteworthy that an estimate of the passband limit based upon the requirement of complete correlation of speckle images in adjacent wavelengths, gives the value $\Delta\lambda \sim 5\text{nm}$ for the 6m telescope.

Similar estimates can also be made for the correlation region size for two point sources separated by angle α . Simulation of non-isoplanicity effects was accomplished with a coherent optical processor. The atmosphere was simulated by a thin phase medium, placed at some equivalent distance H from a telescope. If $f(\xi, \eta)$ is the light field at an aperture from source 1, then the field from source 2 will be $f(\xi + \alpha H, \eta)$. In accordance with eq. (1), images of these point sources can be represented as:

$$\begin{aligned} g_1(x, y) &= |m(x, y)|^2 + m(x, y) n_1^*(x, y) + m^*(x, y) n_1(x, y) + |n_1(x, y)|^2 \\ g_2(x, y) &= |m(x, y)|^2 + m(x, y) n_2^*(x, y) + m^*(x, y) n_2(x, y) + |n_2(x, y)|^2 \end{aligned} \quad \text{---(2)}$$

where $m(x, y)$ is the Fourier transform of the light field inside the region for which coincidence of phase distortions takes place, $n(x, y)$ is the Fourier transform of the light field outside this region. According to (2) complete correlation exists within distances $\alpha H < r_0$, where r_0 is the radius of the light wave correlation at the aperture. Due to interference, correlation decreases rapidly with distance but by our estimates substantial correlation remains up to $\alpha H \leq 0.1D$. Taking this into account and in accordance with Hubbard et al. (1979), where the size of the isoplanatic patch for a 2.3m telescope was found to be $6''$ in typical conditions, 15 arcsec isoplanicity can be expected for the 6m telescope.

6. CONCLUSIONS

1. The estimates of atmospheric parameters made in section 5 are of importance for determining the general limitations of speckle interferometry techniques and can also be useful for designing multiple

mirror telescopes.

2. With the accuracy and sensitivity of the speckle system under review, realization of the following scientific programme can be expected: (a) measurements of angular diameters of red semi-regular, and Mira variables in the continuum and in TiO absorption bands, synchronously with spectrophotometry or VRI photometry; (b) measurements of close visual binaries, spectroscopic binaries and stars with composite spectra, and also the search for new systems accessible within the 6m telescope diffraction limit.

3. An absolute internal error as small as 0.001 arcsec for binary separations makes it possible to measure variations in the separation distance with a view to detecting gravity disturbances caused by invisible massive objects.

REFERENCES

- Chernyj, V.G. 1980, *Astron. Tsirk.* No.1133, pp. 4-5.
- Dudinov, V.N., Erokhin, V.N., Kuz'menkov, S.G., Rylov, V.S., Tsvetkova, V.S. and Shabanov, M.F. 1979, *Doklady Akad. Nauk, USSR, Ser. "A"*, No.7, pp. 550-554.
- Dudinov, V.N., Erokhin, V.N., Konichek, V.V., Kuz'menkov, S.G., Rylov, V.S. and Tsvetkova, V.S. 1980, *Astron. Tsirk.* No.1134, pp. 4-6.
- Dudinov, V.N., Tsvetkova, V.S., Kryshtal', V.A., Gurenko, A.N. and Shpilinskii, L.F. 1977, *Vestn. Khar'kov Univ.* No.160, pp. 65-76.
- Dudinov, V.N., Tsvetkova, V.S., Kuz'menkov, S.G. and Konichek, V.V. 1979, *Vestn. Khar'kov Univ.* No.190, pp. 16-24.
- Finsen, W.S. and Worley, C.E. 1970, *Republ. Obs. Johannesburg Circulars*, Volume 7, No.129, pp. 203-254.
- Hubbard, G., Hege, K., Reed, M.A., Strittmatter, P.A., Woolf, N.J. and Worden, S.P. 1979, *Astron. J.* 84, pp. 1437-1442.